A Study of the Δ^{33} S Signature of Xenoliths from the Premier Kimberlite, South Africa

Greg Polley

Geol394H

 $Dr.\ Sarah\ Penniston-Dorland\ \&\ Dr.\ James\ Farquhar$

November 23, 2011

1 Introduction

South Africa hosts the largest layered igneous intrusion and platinum-group element (PGE) repository in the world, the Bushveld Complex. Emplaced at roughly 2.05 Ga within the Kaapvaal craton, the magma sources of this complex have been widely debated (Richardson and Shirey, 2008). Although the magma itself is thought to be derived from the mantle, previous isotopic analyses of oxygen, strontium, neodymium, and osmium suggest significant amounts of crustal contamination. Measurements of non-zero Δ^{33} S for Bushveld igneous rocks also suggest contamination (Penniston-Dorland et al., 2008). Models to explain these anomalous isotopic signatures include contamination of magma by upper crust upon emplacement, contamination by the sub-continental lithospheric mantle (SCLM), and contamination of magma by lower crust in a lower crustal staging chamber (Shiffries & Rye, 1989; Richardson and Shirey, 2008; Harris et al., 2004).

Figure 1 depicts a cross section of the Earth's crust and upper mantle, demonstrating the possible contamination reservoirs that could have supplied the Bushveld Complex with its anomalous isotopic signatures. The color scheme transitions from cool colors representing low Δ^{33} S values (asthenosphere = blue = Δ^{33} S of 0) to warmer colors representing high Δ^{33} S values. The middle of the SCLM has purposefully been left vacant of peridotite and eclogite xenoliths, implying that they have been moved by the kimberlite eruption (derived from asthenospheric magma) and brought to the surface of the crust and deposited within the Bushveld Complex. The juvenile mantle is thought to possess a Δ^{33} S signature of zero; however, only a small suite of mantlederived samples has been investigated for multiple sulfur isotopic composition.

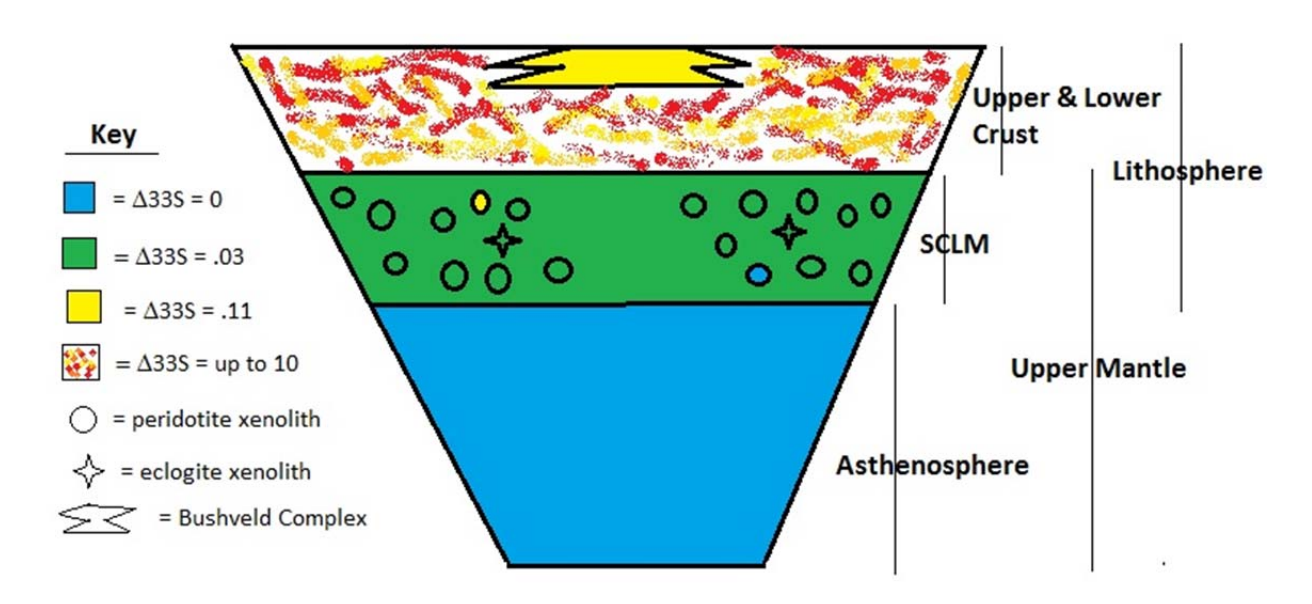


Figure 1 Cartoon of a cross section of Earth's crust and upper mantle. Color coded with Δ^{33} S values of each reservoir. Not drawn to scale.

Samples for this study came from the Premier kimberlite pipe, located centrally within the Kaapvaal craton and Bushveld Complex. This site was chosen due to its spatial and temporal correlation with the Bushveld Complex. The peridotite and eclogite xenoliths have about the

same age as the emplacement of the Bushveld Complex, which is around 2.05 Ga (Richardson & Shirey, 2008). This implies that as these rocks were at rest in the sub-continental lithospheric mantle, an asthenosphere-derived magma source erupted through the SCLM. This magma melted the xenoliths, and allowed for them to record a new age once they recrystallized. This new age is consistent with the emplacement age of the Bushveld Complex, and therefore these xenoliths are thought to sample the original magma source of the Bushveld complex. At around 1.18 Ga, a kimberlite eruption extracted many of these xenoliths and transported them to the surface of the crust. This eruption is known as the Premier kimberlite, and from these xenoliths we hope to elucidate the original magma source and source of isotopic contamination of the Bushveld Complex.

The hypothesis of this project is that mantle-derived xenoliths from the Premier kimberlite have a nonzero $\Delta^{33}S$ isotopic signature. If this hypothesis is supported by data, then the ultimate contamination source of the magma for the Bushveld may also be constrained. This may then imply that the original source of contamination seen in the Bushveld may be from the subcontinental lithospheric mantle, incorporating the anomalous isotopic signatures as the magma rose through this area of the upper mantle. This project provides a better understanding of the source of the Bushveld magma, the composition of the underlying mantle, and how the Bushveld acquired a mass independent sulfur isotopic composition.

2 Geological Setting

2.1 Kaapvaal Craton

The Kaapvaal craton is host to the largest known gold and platinum deposits as well as significant diamond deposits in surrounding kimberlite pipes. The craton covers an area of approximately 1.2 million km² and is connected to the Zimbabwe craton to the north by the Limpopo belt. It is flanked by Proterozoic orogens to the south and west, and to the east by the Lebombo monocline (Gregoire et al., 2005). The Kaapvaal craton was formed as a result of the amalgamation of the Witwatersrand (~3.7 Ga old) and Kimberley (~3.2 Ga blocks by subduction accretion and

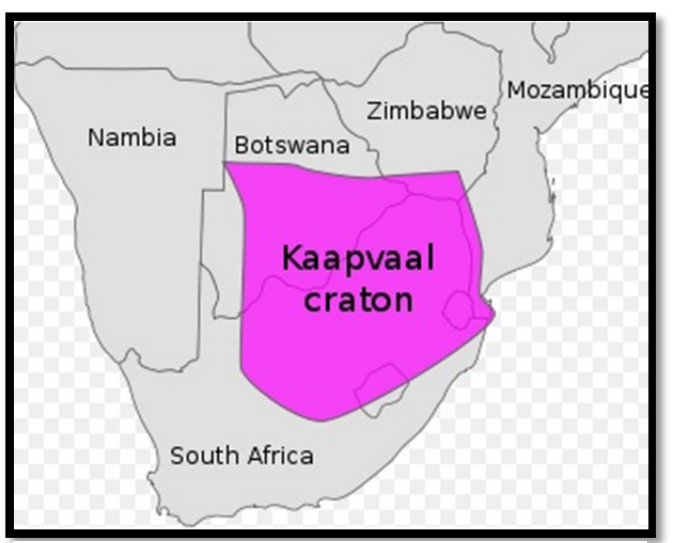


Figure 2 Map of southern Africa, displaying the Kaapvaal craton and its relation to modern day countries old)

continent-continent collision around 2.9 Ga ago (Richardson & Shirey, 2008). Subsequently, the newly formed craton collided with the Zimbabwe craton around 2.5-2.7 Ga ago, producing the Limpopo belt. Archean crust within the central zone of this belt then experienced a second major tectonothermal event around 2.0 Gyr ago, overlapping the well constrained 2.054 Gyr emplacement age of the Bushveld Complex. The Kaapvaal craton is a mixture of early Archean

granite-greenstone and older tonalitic gneisses, intruded by various granitic plutons, overlain by late Archean basins filled with sequences of volcanic and sedimentary rocks.

2.2 Bushveld Complex

The Rustenburg Layered Suite of Bushveld Complex in South Africa is the world's largest mafic-ultramafic layered igneous intrusion, covering an area of nearly $66,000 \text{ km}^2$. The stratigraphy of the intrusion can be divided into a basal Marginal Zone, overlain by Lower Zone, Critical Zone, Main Zone, and Upper Zone. The formation of the Bushveld Complex is still a debated topic, but most authors agree that the

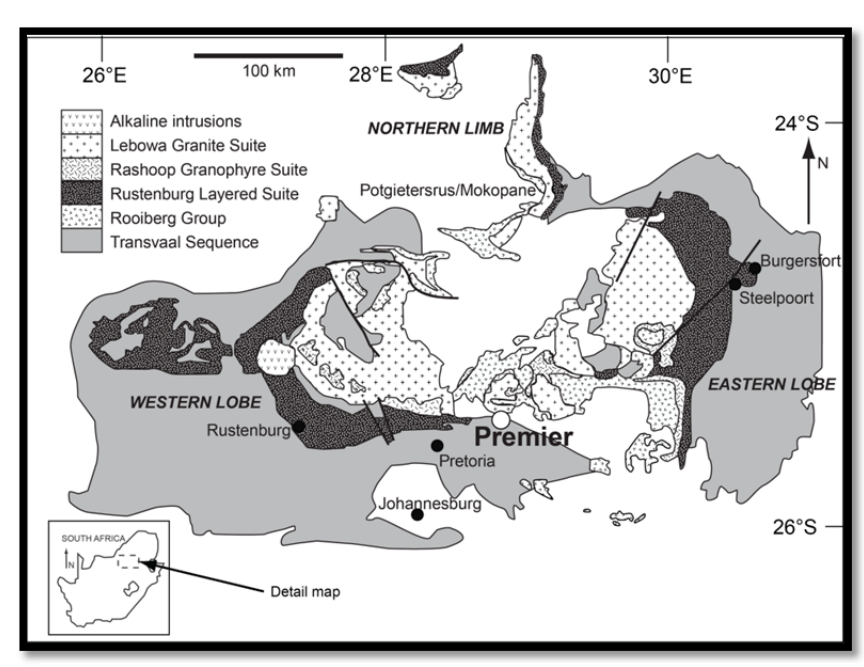


Figure 3 Map showing the spatial relationship between the Premier kimberlite pipe and the Bushveld Complex, South Africa.

enormous volume of magma produced by the Bushveld magmatism was connected to the emplacement of a mantle plume. This mantle plume's source was most likely deep beneath the lithosphere of the Kaapvaal craton, resulting in metasomatism and refertilization of the mantle. The origin of the unusual characteristics of the Bushveld Complex is still ambiguous, whether they are related to crustal contamination or partial melting of enriched mantle lithosphere, and whether the complex was formed by intrusion and solidification of multiple pulses of magma or was one open system through which magmas passed to the surface (Hatton & Sharpe, 1989; McCandless et al., 1999; Maier et al., 2000).

What is less clear is whether the SCLM could possibly have been responsible for the non-zero Δ^{33} S in the Bushveld Complex. This project will attempt to answer that question using multiple sulfur isotope analyses, and ultimately provide a better understanding of the source of isotopic contamination in the Bushveld Complex.

2.3 Premier Kimberlite

The Premier kimberlite pipe is located centrally within the Kaapvaal craton, about 50 km east of Pretoria, South Africa. It is the largest of the kimberlites erupted on the Kaapvaal craton, with an emplacement age of 1179 ± 36 Ma (Smith, 1983). It is one of twelve intrusions near the town of Cullinan, and hosts numerous eclogite and peridotite xenoliths suitable for sulfur isotopic analysis. This pipe intruded dolomite, shale, and quartzite of the Transvaal Sequence, norite of the Main Zone of the Bushveld Complex, Rooiberg felsite, and Waterberg quartzite and conglomerate (Maier et al., 2005). Since emplacement however, the uppermost 300 m have been eroded away. The Premier hosts various kimberlite phases, including tuffistic kimberlite breccia, hypabyssal kimberlite, and aphanitic dykes.

The mantle xenolith suite from Premier contains abundant garnet peridotites, lesser quantities of spinel peridotites, igneous textured xenoliths with hydrous minerals, and common Cr-poor megacrysts (Gregoire et al., 2005). It is also host to ecologite xenoliths. However, as seen in Figure 1, peridotite xenoliths are much more abundant than eclogite xenoliths within this particular kimberlite. The most common types of xenoliths from the Premier kimberlite are garnet and spinel harzburgites and garnet lherzolites. The Re-Os systematics of the peridotite of this area are similar to those of kimberlite borne xenoliths from the Kaapvaal lithospheric mantle that have very low Re/Os and ¹⁸⁷Os/¹⁸⁸Os (Carlson et al., 2000).

3 Sulfur Isotope Systematics and Notation

Sulfur is the tenth most abundant element in the universe and the 14^{th} most abundant element within the Earth's crust. It has a total of five naturally occurring isotopes, including 32 S, 34 S, 35 S, and 36 S. Four of these are naturally occurring stable isotopes, while the fifth (35 S) is unstable, or radiogenic. Stable isotope geochemistry focuses on variations in the relative abundances of stable isotopes among substances. The difference in partitioning of various isotopes, also known as fractionation, is due to equilibrium and kinetic effects. Isotope ratios are usually expressed as the ratio of a minor isotope of an element to a major isotope of the element. For sulfur isotopes, 34 S/ 32 S is the ratio most commonly measured. Most fractionation processes will cause slight variations in these ratios to the fifth or sixth decimal places; since these variations are so small, we express the isotopic composition of a substance by using delta notation, as variation in parts per thousand relative to a reference material. The δ -notation is used to describe 34 S/ 32 S and is written as:

$$\delta^{34}S = \left(\frac{\left(\frac{34S}{32S}\right)_{\text{sample}} - \left(\frac{34S}{32S}\right)_{\text{reference}}}{\left(\frac{34S}{32S}\right)_{\text{reference}}}\right) \times 1000$$

which is in units of ‰, or permil. The reference material used for sulfur isotopes is Vienna Canyon Diablo Troilite (VCDT) with $\delta^{34}S = 0.0\%$ by definition. Current measurements are made relative to a silver sulfide reference material IAEA-S-1 which has a $\delta^{34}S$ value of -.3‰ since the supply of Canyon Diablo Troilite material has been exhausted (Krouse & Coplen, 1997). The selection of a meteoritic sulfide phase as a reference for sulfur is useful because it is thought to represent the primordial sulfur isotopic composition of the Earth. Therefore, any variation in the isotopic composition of terrestrial sulfur relative to VCDT reflects differentiation since the formation of the Earth.

For sulfur, ³⁴S/³²S is the ratio most commonly measured when studying terrestrial systems. This ratio was chosen because it reflects the two most abundant isotopic forms of the element, and also because isotopic fractionation is governed by mass such that different isotopic ratios will vary systematically with one another consistent with the mass differences between the isotopes (Vaughan, 2006). The variations in ³³S/³²S ratio of a sample will be about half that of ³⁴S/³²S because the difference between ³³S and ³²S is one half the difference between ³⁴S and ³²S. Following the same principle, variations for ³⁶S/³²S will generally be twice that of the ³⁴S/³²S

ratio. This linear fractionation trend is known as "mass-dependent fractionation". Mass-independent fractionation, on the other hand, is reflected by non-linear variations in isotopic fractionation with mass.

On a plot of one isotopic ratio versus another, such as δ^{33} S against δ^{34} S, samples that have undergone mass-dependent fractionation fall along a line known as a mass-fractionation line, the slope of which corresponds to the relative mass difference between the two ratios, as seen in figure 2. Deviations from this line reflect mass independent fractionation processes. For sulfur isotopes, these deviations may be expressed as Δ^{33} S and defined mathematically by:

$$\Delta^{33}S = \delta^{33}S - 1000 \left(\left(1 - \frac{\delta^{34}S}{1000} \right)^{.515} - 1 \right)$$

where .515 is the approximate slope of mass-dependent behavior on the δ - δ diagram, and characterizes all biological and non biological fractionation processes except photochemical processes (Hiebert & Bekker, 2010).

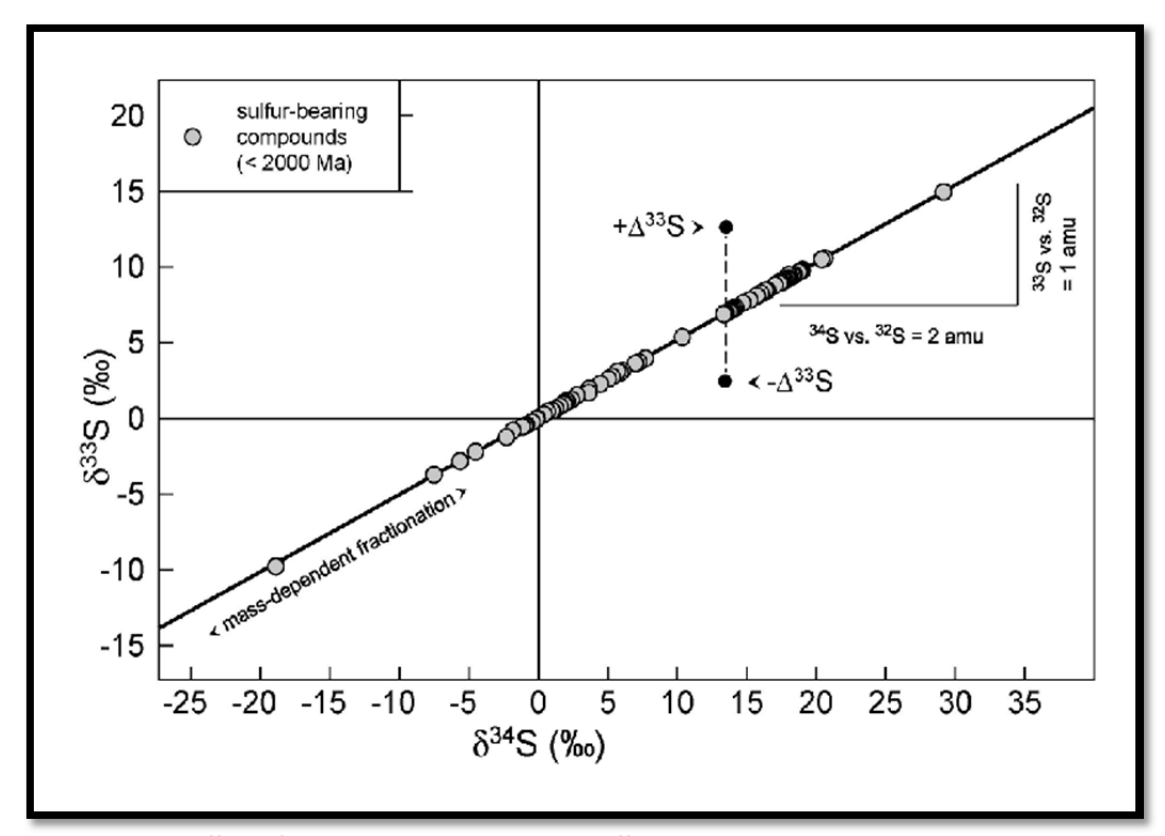


Figure 4 Plot of δ^{33} S vs δ^{34} S with mass fractionation line; Δ^{33} S is reported as the deviation from this line.

Geochemical processes, the most notable of which are oxidation and reduction, significantly fractionate sulfur isotopes away from bulk-Earth values in geological systems. Oxidation produces ³⁴S enriched-species relative to reactants, whereas reduction produces species that are depleted in ³⁴S. Most isotopic fractionation is controlled by variations of thermodynamic

properties of molecules that are dependent on mass. Isotopic fractionation is usually governed by equilibrium or kinetically controlled chemical or physical processes (Vaughan, 2006). Important equilibrium processes are isotopic exchange reactions, which redistribute isotopes to new substances. Equilibrium isotope effects result from the effect of atomic mass on bonding; this means that molecules with a heavier isotope are more stable than those with a lighter isotope. Kinetic processes include irreversible chemical reactions such as bacterially mediated processes like some enzymatic steps in sulfate reduction, and physical processes such as evaporation and diffusion. A few factors that mediate the magnitude of equilibrium stable isotope fractionation are temperature, chemical composition, crystal structure, and pressure (Vaughan, 2006). Pressure is a negligible parameter at upper crustal conditions. Isotopic fractionation can also be related to chemical variables such as oxidation state, ionic charge, atomic mass, and electronic configuration of the isotopic elements. The effect of oxidation state is especially important

because higher oxidation states of sulfur are enriched in the heavier isotopes relative to lower oxidation states.

Photochemical processes in the upper atmosphere have been found to cause massindependent fractionation in sulfur isotopes. The origin of some anomalous Δ^{33} S values is attributed to atmospheric photochemistry involving sulfur dioxide in a primitive atmosphere with reduced oxygen and ozone and increased ultraviolet transparency (Farguhar et al., 2002). Prior to 2.4 Ga, sulfide and sulfate in rocks from various geologic settings have anomalous signatures, with Δ^{33} S values ranging from -2.5 to 10%. Rocks younger than 2.4 Ga generally have Δ^{33} S = 0 (+ 0.2)‰. There is an abrupt change in magnitude of anomalous mass-independent fractionation around 2.4 Ga which has been interpreted to reflect the development of an oxygenated atmosphere. The development of an ozone layer would have shielded lower parts of the atmosphere from photochemical processes induced by

Measurements of elevated $\Delta^{33}S$ values of Bushveld igneous rocks by Penniston-Dorland et al. (unpublished results, 2008) have shown non-zero $\Delta^{33}S$ in Bushveld igneous rocks as seen in Figure 6. MORB $\Delta^{33}S$ values are used as

ultraviolet radiation

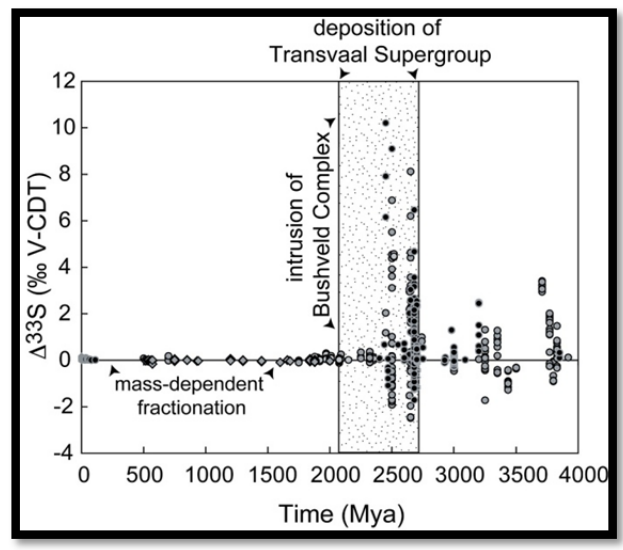


Figure 5 Age distribution of sulfur isotope anomalies in sedimentary rocks (Farquhar et al., 2000).

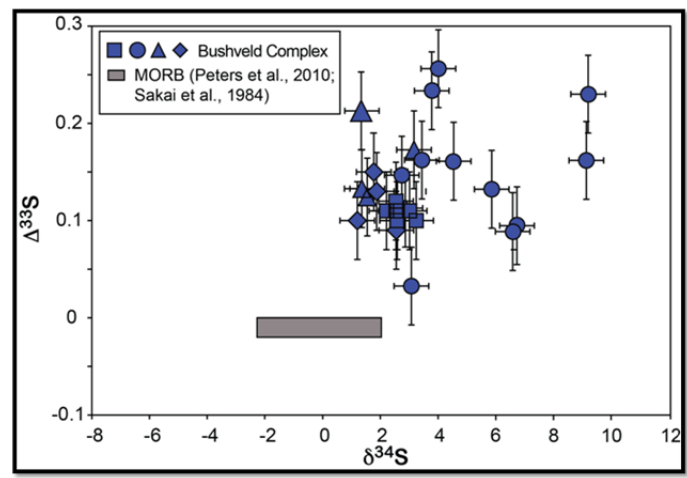


Figure 6 Nonzero Δ^{33} S values of Bushveld igneous rocks, with mantle xenolith values from Kilbourne Hole for reference.

a proxy for asthenospheric mantle measurements ($\Delta^{33}S = 0$), and are depicted as the gray box on the graph. These results suggest that the Bushveld magma became contaminated at some point along its ascent or that the mantle source already attained the signature.

4 Sample Description

4.1 Hand Samples

Xenoliths for this study were selected from the collection of F.R. Boyd at the Smithsonian National Museum of Natural History, who collected these samples from the Premier Mine, South Africa. Requested and received were 12 peridotite xenoliths, 3 eclogite xenoliths, and 3 kimberlite samples; however, not all of these samples were used for this project. The peridotite samples include eight harzburgites, two lherzolites, and two dunites. Five of these samples were accompanied by a thin section. The mass of the peridotite samples fell between the range of 45 to 80 grams. The eclogite xenoliths and kimberlite samples were relatively smaller, between 15 and 25 grams. Various large phenocrysts are visible in hand sample, including garnet, bronzite (an Fe²⁺-enriched variety of enstatite), and diopside for the peridotites, whereas garnet and omphacite were clearly visible in the eclogites. A full list of the samples used for this project is seen below in Table 1. As seen, data was only collected from eight of the twelve peridotite samples, one of the three eclogite samples, and zero of the three kimberlite samples. A further discussion of the analysis of these samples will be described later.

Sample ID	Rock Type	Analysis	Samp	le ID	Rock Type	Analysis
FRB 1656*	Garnet		FRB	908 D 1	Eclogite	
	harzburgite	No				No
PHN 5239	Garnet		FRB	908 D2	Eclogite	
	harzburgite	Yes				Yes
FRB 1318	Garnet		FRB	908 D3	Eclogite	
	harzburgite	Yes				No
FRB 1657*	Garnet		FRB	1367-14	Kimberlite	
	harzburgite	No				No
FRB 1352	Garnet Iherzolite		FRB	1367-21	Kimberlite	
		Yes				No
FRB 1309*	Garnet Iherzolite		FRB	900C-2	Kimberlite	
		No				No
FRB 1370	Phlogopite dunite	Yes				
FRB 1331.3	Spinel dunite	Yes		*Accom	panied by thin se	ection
FRB 1375	Spinel-graphite-			Accomp	ounica by thin se	ction
	phlogopite					
	harzburgite	No				
FRB 1659*	Spinel harzburgite	Yes				
FRB 1655*	Spinel harzburgite	Yes				
PHN 5247	Spinel harzburgite	Yes				

Table 1 Complete list of samples acquired and used for this project

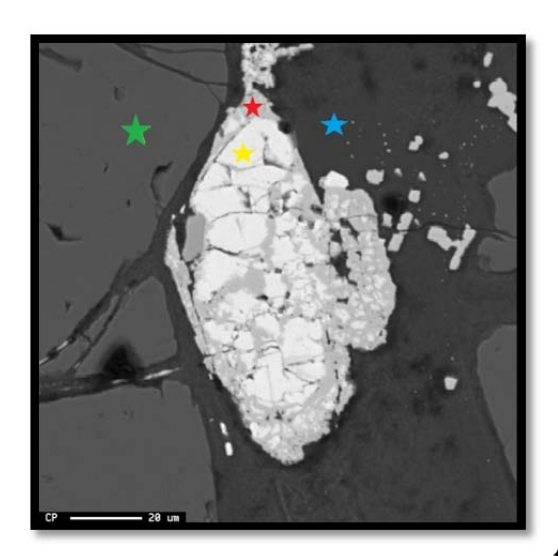


Figure 7 BSE image of sample FRB 1659 shows pentlandite (yellow star), along with associated phases olivine (green star), serpentine (blue star), and iron oxide (red star). Scale bar of 20 um shown at bottom left corner of image.

4.2 Thin Section Analysis

Using the petrographic microscope and electron microprobe, common and accessory minerals were identified. Mineral phases include olivine, garnet, orthopyroxene (var. bronzite), and spinel, with the spinel species usually being chromium-bearing. Sulfide minerals occur as trace in each thin section; among those identified include pentlandite ((Fe, Ni)₉S₈), millerite (NiS), and pyrrhotite (Fe_{1-x}S). Other accessory mineral phases include magnetite, calcite, serpentine, barite, and celsian. Thin sections have been analyzed using electron dispersive spectrometry (EDS) on the electron microprobe in order to confirm the presence of both common and trace minerals within the xenoliths.

4.2.1 Spinel Harzburgite

Mineral phases that were opaque in transmitted light in thin section FRB 1659 and FRB 1655 were investigated using electron dispersive spectrometry (EDS) on the electron microprobe. In thin section, sample FRB 1659 had noticeably large opaque phases; unfortunately, these were not sulfide phases but rather chromium rich spinel. Two distinct sulfide phases were observed in sample FRB 1659; pentlandite ((Ni, Fe) $_9$ S₈) and millerite (NiS). Sample FRB 1655 had

pentlandite along with an interesting assemblage of minerals that are likely secondary. A small patch of barium-rich minerals was found which comprised barite (BaSO₄) and celsian (barium feldspar, BaAl₂Si₂O₈). Iron oxide was also noticed in both thin sections as a product of alteration.

4.2.2 Garnet Harzburgite

Opaque minerals found within the garnet harzburgites include also chromium-rich spinel phases, iron oxides, and sulfides. FRB 1656 contained only millerite, while FRB 1657 contained only pentlandite. Another accessory mineral phase found within FRB 1656 was calcite.

4.2.3 Eclogite

Although no thin sections were available for the eclogite samples, the characteristic garnet and omphacite of these metamorphic rocks are clearly visible as garnet and omphacite. One of the

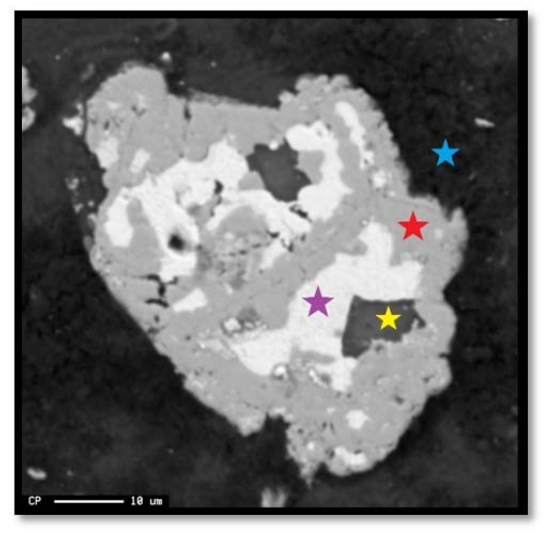


Figure 8 BSE image of sample FRB 1656 shows sulfide phase millerite (purple star) in association with phases calcite (yellow star), serpentine (blue star), and iron oxide (red star). Scale bar of 10 um shown at bottom left corner of image.

samples (FRB 908 D3), however, has been cut to show a visible sulfide grain. Upon further investigation using the electron microprobe, the phase was confirmed to be rich in nickel and sulfur, and most likely to be millerite. Millerite is not a stable mineral found within the mantle.



Figure 9 Eclogite sample FRB 908 D3 with visible sulfide crystal circled in yellow. Quarter shown for scale

4.2.4 Kimberlite

Kimberlite is a type of volcanic rock that formed deep within the mantle. Formation depths range from 150 to 450 km, and kimberlite eruptions are rapid and violent, often comprising a considerable amount of volatile material. Kimberlite is most likely derived from greater depths than any other igneous rock type; this implies that it has potential to provide information about the

The upper limit for millerite stability is 379 °C (Vaughan, 2006), which is cooler than what is expected for the mantle. This means that the nickel sulfide is either an alteration product when the xenolith became emplaced, or that the nickel sulfide phase originally in the mantle became unstable and retrograded to a more stable phase in a cooler temperature environment. Regardless, this provided clear evidence that there would be enough sulfur in the eclogite xenoliths to perform the proper chemical reactions.



Figure 10 Kimberlite sample FRB 1367-14. Quarter shown for scale.

composition of the deep mantle and about the interface of the continental lithosphere and the underlying asthenosphereic mantle. Because it commonly entrains eclogite and peridotite xenoliths and transports them to the surface of the crust, analyzing this material may help to provide a better understanding of how they are related and if they have interacted with each other upon ascent.

5 Analytical Methods

5.1 Pulverization

A portion ranging from a quarter to a half of each xenolith sample was cut using the rock saw (~15-30 g). This piece was then crushed using a steel mortar and pestle, breaking down the rock into finer grains and powder. Another option to attain fine powder is to use a shatterbox;



Figure 11 Steel mortar and pestle

however, I chose to forgo this technique for two important reasons. Firstly, the sample masses that were crushed are less than the amount needed to properly run the shatterbox. Secondly, with such vigorous vibration and movement, this technique will likely add external heat to the sample, possibly oxidizing or otherwise negatively influencing sulfur bearing species within the rock. Therefore, after the sample was crushed using the steel mortar and pestle, it was then transferred to a smaller, ceramic mortar and pestle to achieve a fine powder texture. Cleaning between samples consists of washing the mortar and pestle with water, and then grinding sand to cleanse the apparatus.

5.2 Chemistry - CRS

Once fine powder was created, sulfur extractions were then carried out. This process was performed within the Stable Isotope Lab in the Chemistry building. The procedure involves reacting the fine-grained samples with HCl and a CRS (chromium reducing solution) solution. The hydrochloric acid is used to extract acid volatile sulfur (or elemental sulfur) whereas the chromium reducing solution isolates sulfur from sulfide phases within the rock. Since both of these reagents will be added simultaneously to the samples, sulfur from both phases (elemental and sulfide) will be liberated as H₂S and trapped as either silver sulfide (using silver nitrate). For each sample, 15 mL of CRS solution and 15 mL of HCl are injected into the reaction flasks, and then heated. As nitrogen is pumped into the flask, both elemental sulfur and sulfur from sulfide phases is liberated as H₂S and becomes trapped in a solution of 15 mL of MQ water, 2 mL of HNO₃, and 2 mL of AgNO₃. The sulfur then recombines to form silver sulfide, and is precipitated out of the solution. This type of reduction is colloquially known as a CRS reduction. For the initial suite of samples sulfur was extracted from 1 g of powdered rock sample to determine the sulfur concentration of the xenoliths and to adjust the mass reacted accordingly thereafter.

5.3 Chemistry – Thode

Thode reductions were also performed on several of the samples, and at least one sample from each rock type (peridotite, eclogite, kimberlite) had undergone a Thode reduction. This type of reaction is set up similarly to the CRS reduction; however, the solution used to react with the sample is different. Instead of chromium chloride solution, 30 mL of a mixture of hydrochloric acid, hydrophosphorous acid, and hydroiodic acid is added to the reaction vessel with the powdered sample. This solution liberates all sulfur from sulfate phases, and traps the sulfur as silver sulfide, just like the CRS reduction.

5.3 Sample Cleaning

About a week after sulfur extraction, the samples must then be cleaned using ammonium hydroxide (NH₄OH) and milli-Q (MQ) water. Excess solution (supernatant) must be poured out and disposed of properly, and then MQ water is added to the product and poured into a centrifuge tube. The tube is shaken and then filled to 45 mL with MQ water. The centrifuge must then be run at 5000 rpm for 5 minutes. Once samples have been centrifuged, the excess water is decanted; the tube is then filled with 10-15 mL of MQ water, shaken, and then filled to 45 mL. The sample is then centrifuged again, and this process must be repeated for a third time. After

the third centrifuge, the tube must be filled with 10-15 mL of NH₄OH solution, shaken, and then filled to 45 mL with the NH₄OH. After they are centrifuged, samples must then be left overnight. The following day, the samples may be decanted, washed with MQ, filled to 45 mL, and centrifuged twice. The pellet after this process is then pipetted into a micro centrifuge tube, and may sit in either a warm oven or covered in aluminum foil (to prevent contamination). The sample will then be dry and ready for fluorination and mass spectrometry.

5.4 Sulfur Concentration

After the samples had been dried, the mass of the silver sulfide that was produced from the CRS reduction was determined. Using this number, and the mass of the initial rock powder that was reacted, a concentration of the amount of sulfur within the rock can be determined. The equation that was used is

$$Mrp = \left(\frac{(Mms * Saw)}{(Ag2Saw * Crp) * 1000}\right) * 10^6$$

Where M_{rp} is mass of rock powder (in grams), C_{rp} is sulfur concentration in rock powder (in ppm), S_{aw} is sulfur atomic weight (in gram/mole), Ag_2S_{aw} is atomic weight of silver sulfide (in gram/mole), and M_{ms} is mass required for mass spectrometry measurement (in mg).

5.5 Fluorination and Mass Spectrometry

The silver sulfide product that has been cleaned and dried is reacted with F_2 to form SF_6 , which is purified for mass spectrometric analysis. Converting the sample from silver sulfide to gaseous SF_6 form, rather than SO_2 , has two advantages. First, it is an inert, non-absorbing gas, and second

there is no ambiguity in isotopic speciation since fluorine has a single stable isotope (Vaughan, 2006). For mass spectrometry, the gas molecules are ionized to positively charged particles which are accelerated through a voltage gradient. The ion beam passes through a magnetic field, which causes separation of various masses. In conventional dual-inlet mass spectrometers, a sample gas is measured alternately with a reference gas. The beam currents are measured in faraday cups and can be related to the isotopic



Figure 12 Mass spectrometer used to attain multiple sulfur isotope data

ratio when the sample and standard gases are compared (Vaughan, 2006). Once

these processes have been complete, the δ values of each sample are calculated.

6 Results

6.1 Preliminary Data

Sample BHTV1.1 was chosen as an internal standard in order to demonstrate reproducibility and gauge the uncertainty of the whole process from extraction to measurement. Since the overall sulfur concentration for this sample was unknown, the amount of whole rock needed to reduce was also unknown. A line was reduced using five different masses each of the same sample BHTV1.1. The masses were 50 mg, 500 mg, 1 g, 5 g, and 20 g. The results of this reduction yielded very little amount of product in the 50 mg and 500 mg samples, whereas the 1 g, 5 g, and 20 g samples all had noticeable product. The samples were then cleaned and dried, and because the combined mass of the samples was relatively low, each was combined into one accumulated mass.

The BHTV1.1 sample was fluorinated and sent over to the mass spectrometer for multiple sulfur isotopic composition analysis. The resulting data is reported in the chart below, along with previously measured isotopic values by Dr. Penniston-Dorland.

Sample / STDV	δ^{33} S	$\delta^{34}S$	δ^{36} S	Δ^{33} S
BHTV1.1 (GP)	0.853	1.413	2.540	0.125
1 σ (GP)	0.011	0.011	0.230	0.011
BHTV1.1 (PD)	0.820	1.339	2.830	0.131
1 σ (PD)	0.148	0.286	0.548	0.013

Table 2 Multiple sulfur isotope composition of BHTV1.1 standard material, measured by Greg Polley (GP) and Dr. Penniston-Dorland (PD). All isotope values have been normalized to VCDT.

The BHTV1.1 sample that I had reduced and sent through to mass spectrometry yielded very similar results to those previously measured by Dr. Penniston-Dorland. Each of my isotope values are within one standard deviation of the measurements that have already been made, thus indicating consistency and accuracy. By acquiring isotope values from a standard, I have successfully shown that I can process samples all the way to mass spectrometry and obtain results that are consistent with previously measured values. Each xenolith sample was processed in the same manner.

6.2 Results

Sulfur was extracted from eight of the twelve peridotite xenolith samples and one of the three eclogite samples via CRS (chromium reducible sulfur) reductions. The product from these reactions was fluorinated to form SF₆, and this compound was then sent through a mass spectrometer for multiple sulfur isotope analysis. The data obtained, which can be seen in Table 3, reveals interesting information and implications in regards to the host magma from which it

came. These data values are reported as % V-CDT (Vienne Canyon Diablo Troilite), using IAEA-S1 as a standard for our lab.

	δ^{33} S	δ^{34} S	Δ^{33} S
FRB 1370	090	261	.044
FRB 1659	1.253	2.367	.035
FRB 1352	386	796	.024
PHN 5239	-2.681	-5.186	007
PHN 5247	-2.001	-4.161	.144
FRB 1318	-1.934	-3.797	.023
FRB 1331.3	2.232	4.35	006
FRB 1655	-1.864	-3.656	.02
FRB 908 D2	-3.952	-7.675	.009
Average	-1.047	-2.091	.032

Table 3 Data values reported for δ^{33} S, δ^{34} S, and Δ^{33} S for eight peridotite xenoliths and one eclogite xenolith (FRB 908 D2).

The $\Delta^{33}S$ values from these mantle-derived xenoliths show both nonzero values and values within analytical uncertainty (error bars for SMAR points represent deviation of \pm .009‰). However, the samples that fall within analytical uncertainty of zero ($\Delta^{33}S = .009, -.006, -.007$) all fall outside of the range of $\delta^{34}S$ values from MORB measurements used to represent the mantle. Although the first hypothesis of the project has been rejected, the fact that these measurements fall outside of the range of $\delta^{34}S$ measurements still may imply contamination from another source, whether it is from eclogitic sub-continental lithospheric mantle or from crustal interactions as these rocks were exhumed. The data however seem to reject the second proposed hypothesis, that the anomalous Bushveld signature developed from the sub-continental lithospheric mantle, as will be discussed in the next section. Although only nine data points have been attained from the possible eighteen, it is important to note that when plotted on a $\delta^{34}S$ vs. $\Delta^{33}S$ plot, all points except for one seem to plot reasonably low on the $\Delta^{33}S$ axis, and this outlier can still be used to either support or reject the second hypothesis of this project using sulfur concentration data.

The range of $\delta^{34}S$ is quite large, ranging from -7.675 to +4.35‰. This may be attributed to inhomogeneity of the SCLM and lower and upper crust as the kimberlite magma ascended, allowing the xenoliths to incorporate different signals along the way. Another explanation is provided by Zheng (1992), who concluded that $\delta^{34}S$ values that are a departure from 0‰ may be attributed to the assimilation of sedimentary sulfide, giving a negative value, or from oceanic evaporite, giving a positive value. Depleted or enriched $\delta^{34}S$ values may be the result of magma degassing; depleted values resulted from SO_4 outgassing while enriched values resulted from H_2S outgassing.

Using the equation described above for determining the concentration of sulfur, an average of about 30 ppm was calculated for the xenoliths. This is nearly at the lower bound for sulfur concentration in xenoliths from the Premier kimberlite; the range of concentrations is from 20 to 450 ppm as reported by Maier et al. (2005). The concentrations determined, however, will prove

important in understanding how these xenoliths and the SCLM are an unlikely source of contamination for the Bushveld Complex.

Figure 13 shows data values in red (peridotite xenoliths) and yellow (eclogite xenolith), plotted along with data values from Bushveld igneous rocks (Penniston-Dorland et al. 2008) and host rocks collected at SMAR (southern mid-atlantic ridge) sites (Peters et al., 2010). I chose to include these other studies on my plot in order to provide significance and a better understanding of what these values actually mean. The SMAR values represent unaltered mantle, comprising a Δ^{33} S value of zero or near zero. The usual range of δ^{34} S values for SMAR samples is -2 to 2 permil, as seen in Figure 13 as the gray box. Each of my data points fall outside of this range, even with analytical uncertainty, and therefore may be deemed as non-zero values. This data is important because it not only tells us that these xenoliths are carrying a contaminated signature, but it also tells us to what extent the xenoliths have been contaminated, and whether or not they may be a likely source of contamination for the Bushveld Complex.

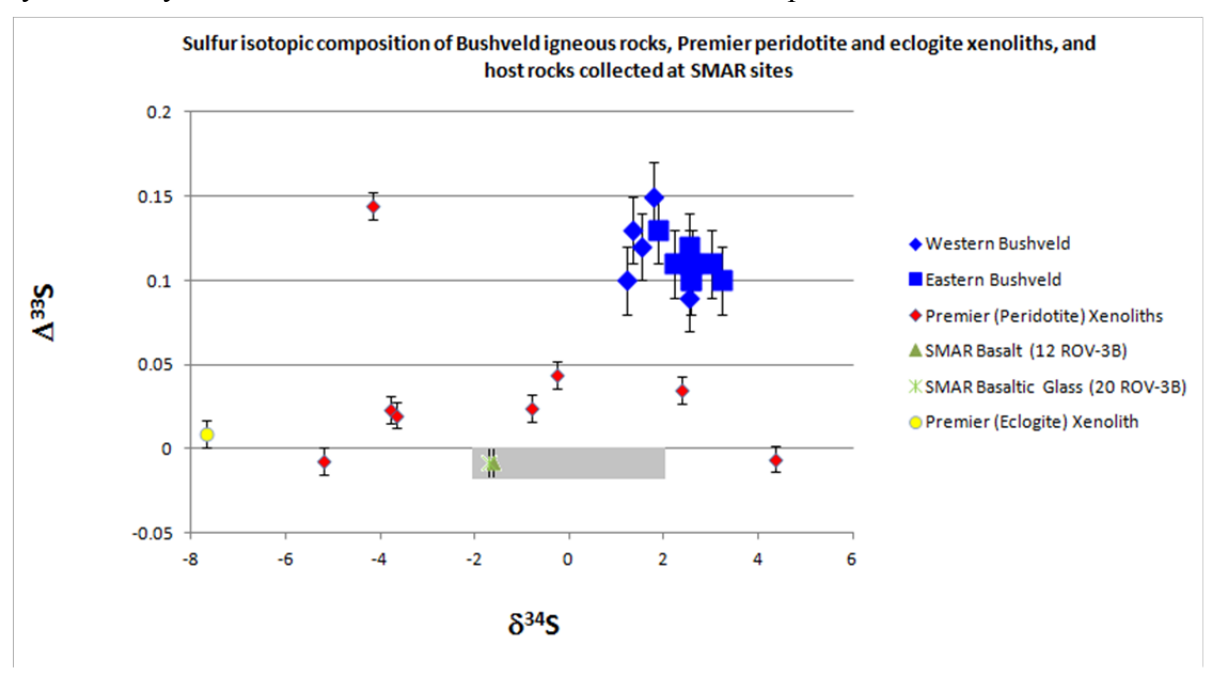


Figure 13 Data points collected for eight peridotite xenoliths and one eclogite xenolith, plotted with Bushveld igneous rock data and SMAR range used to represent mantle values.

Referring back to Table 1, only eight peridotite samples and one eclogite sample had been analyzed. Two of the peridotite samples yeilded negligible (<< 2 mg) silver sulfide product when reacted during a CRS reduction, and even when reacted with a greater mass of powder for a second time, there was still not enough product for isotopic analysis. Two other samples have been reduced and are ready to be fluorinated and sent to the mass spectrometer; however, the data for these points will not be included within this report. The eclogite sample with the visible sulfide grain was decided on to not be included within this study. The other eclogite sample was reduced and is ready to be fluorinated with the other peridotite samples, but once again, the data for this sample will not be included within this study. When reduced via CRS, the kimberlite samples yeilded negligible amounts of silver sulfide, meaning the concentration of sulfur from sulfide phases within these rocks is very low. None of the kimberlite samples were able to

produce data from the CRS reductions; however, one of the samples was reduced using the Thode technique, and interestingly produced enough product to be fluorinated and sent to the mass spectrometer for istotopic analysis. This means that the majority of the sulfur within these kimberlites is stored as sulfate phases rather than sulfide or elemental sulfur. Although product was produced via Thode, all Thode data will not be incorporated into this project, as there was not enough time to run another fluorination and mass spectrometer analysis. All samples that were reduced using Thode can be seen in Table 4.

Type	Sample	Stage
Peridotite	FRB 1352	Ready for fluorination
Peridotite	FRB 1370	Ready for fluorination
Peridotite	FRB 1656	Ready for fluorination
Peridotite	FRB 1655	Ready for fluorination
Eclogite	FRB 908 D1	Ready for fluorination
Kimberlite	FRB 1367-21	Ready for fluorination

Table 4 Samples that have been reduced using Thode reduction technique and are all ready for fluorination and mass spectrometer analysis.

6.1 Evaluation of Significance of Data

In order to evaluate whether the reported values are within uncertainty of zero or not, a t-test will be used. This type of statistical test assesses whether the means of two groups are statistically different from each other. The two groups will be xenoliths with measured values of $\Delta^{33}S$ and the SMAR $\Delta^{33}S$ values. If all the rocks are reported to have only one of these compositions, they will be tested for significance against the control values ($\Delta^{33}S = 0$). The null hypothesis of this project is that the $\Delta^{33}S$ of the xenolith samples from the Premier kimberlite is zero.

The t-test involves a ratio; the top is the difference between the two means and the bottom is a measure of the variability or dispersion within the data. The equation that will be used is as follows:

$$t = \frac{Xt - Xc}{\sqrt{\frac{vart}{nt} + \frac{varc}{nc}}}$$

where var_t and var_c are the variance values for each group, and n_t and n_c are the number of samples in each group. The bottom part of this equation is also known as the standard error of difference.

Once a t-value has been computed, it may then be compared to values in a table of significance to test whether the ratio is large enough to say that the difference between groups is not likely to have been a chance finding. To test significance, three different values will be needed: the alpha level (usually taken to be .05), degrees of freedom (sum of number of samples in each group minus 2), and the t-value. If the t-value is large enough to be significant, it can be concluded that the difference between the means for the two groups is statistically different. This statistical analysis is mathematically similar to a one-way analysis of variance (ANOVA) and a

form of regression analysis, and will all yield identical results. This statistical test was chosen over the others because it is simpler to use give the experimental conditions.

By using this formula, a P value of .0001 was determined, meaning the difference between the two means is extremely statistically significant.

6.2 Analytical Uncertainty

Uncertainty so far has been used by lab measurements in the stable isotope geochemistry lab on standard IAEAS-1. Uncertainty of analysis is \pm .008 based on 56 standard measurements made in the lab. Uncertainty among the SMAR samples used as a reference in my plot was \pm .009.

7 Discussion

Three significant models have been reported within the literature suggesting sources of the Bushveld Complex's anomalous isotopic composition. These include contamination upon emplacement within the Transvaal supergroup, contamination in the lower crust via a staging magma chamber, and contamination from the sub-continental lithospheric mantle (SCLM) (Schiffries & Rye, 1989; Harris et al., 2004; Richardson & Shirey, 2008). Each model will be discussed, and evidence both supporting and rejecting each hypothesis will be provided. Through the use of multiple sulfur isotopes from mantle xenoliths from the Premier kimberlite, this project was able to reject the most likely model, that being that contamination from the sub-continental lithospheric mantle is the ultimate source of Bushveld magma.

7.1 Contamination by upper crust upon emplacement

Schiffries and Rye (1989) reported oxygen isotopic data that imposed new constraints on the magmatic evolution of the Bushveld Complex intrusion. Their conclusions reported several factors that suggested a contaminated source magma, and their model was contamination of the magma upon emplacement. The evidence for this model was δ^{18} O values of the Bushveld Complex that were heavier than the δ^{18} O values of primitive mantle derived magmas. This evidence suggests some mechanism of alteration of the isotopic composition of the magma. Sedimentary country rocks and other potential crustal contaminants have heavier δ^{18} O values than Bushveld Complex. The δ^{18} O values of volcanic country rocks from Transvaal Supergroup are typical of normal mantle derived magmas, showing no anomalous isotopic signature. This suggests that the sub-continental mantle they were derived from is not anomalously enriched in δ^{18} O. According to Schiffries and Rye (1989), parental magmas probably acquired their differing isotopic signatures as a result of variations in the nature and amount of material they assimilated during their ascent through the continental crust. However, this model has several disadvantages. First, the lateral homogeneity of δ^{18} O over the large area covered by the intrusion are unlikely to be a product of local contamination upon emplacement; typically the continental crust will be heterogeneous in nature, and therefore anomalous δ^{18} O values should be heterogeneous as well. Another interesting finding by Harris et al. (2004) is that there was no measured systematic change in δ^{18} O values across the RLS, implying that the intruding magmas must have been already contaminated and well mixed.

7.2 Contamination by lower crust in a staging magma chamber

Sharpe et al. (1986) suggested mantle derived magmas mixed with partially melted crust in a "master AFC" (assimilation accompanied by fractional crystallization) chamber which periodically fed into the Bushveld magma, creating the Rustenburg Layered Suite (RLS). The model proposed by Harris et al. (2005) also requires assimilation to take place in a staging magma chamber situated in the lower to middle crust. Measurements of δ^{18} O values at the RLS, part of the Bushveld Complex, are higher (7.1‰) (Harris et al. 2005) than uncontaminated mantle values (5.7‰) (Eiler, 2001). They propose a means of crustal contamination, which would also explain the high initial Sr isotope ratios of the study area. The lack of any apparent systematic change in δ^{18} O with stratigraphic height suggests that magmas became contaminated before emplacement. Incorporation and mixing of local wall rock would contaminate the magma chamber in a homogenous fashion, and thus supply the magma with its anomalous isotopic signature.

7.3 Contamination by sub-continental lithospheric mantle during ascent of magma

Richardson and Shirey (2008) proposed a model based on their measurements of sulfide inclusions in diamonds entrained in Premier kimberlite host magma, suggesting that the main source of the Bushveld platinum group elements was the mantle rather than the crust. The radiogenic Os and Sr isotope signatures of RLS rocks, along with their elevated δ^{18} O values, have been attributed to crustal contamination. However, the upper crust is heterogeneous on the outcrop scale and would require implausibly thorough mixing of local contaminants to explain the 300 km-scale lateral homogeneity (Richardson & Shirey, 2008). Also, seismic tomography of the Kaapvaal and Zimbabwe cratons shows that P-wave velocities at a depth of 150 km beneath the Bushveld complex are 1.0% to 1.5% lower than those in surrounding lithospheric mantle, suggesting partial melt of the SCLM beneath the Bushveld (James et al., 2001). Also, Re/Os ages of xenoliths (~2 Ga) correlate melt extraction from the SCLM at the time of the Bushveld emplacement.

7.4 Interpretation of Sulfur Isotopic Data

The measured Δ^{33} S values obtained from the peridotite xenoliths, although slightly elevated, fall just outside of the unaltered MORB (Mid Ocean Ridge Basalt; represented as SMAR [southern mid antlantic ridge] data points) values (Peters et al. 2008). Since MORB are formed by asthenospheric mantle, they are thought to have Δ^{33} S values approximately equal to zero and the measurements of the SMAR samples confirm this.

Since these mantle derived xenoliths have non-zero $\Delta^{33}S$ values, this implies that the sub-continental lithospheric mantle contains this anomalous isotopic signature. The question thus becomes whether the SCLM (represented by the xenoliths) might be responsible for the contamination seen in the Bushveld. To answer this, simple contamination mixing calculations are used. Below in Figure 3 are a set of six curves based on $\Delta^{33}S$ values vs. percentage of contaminant. These values were based on the equation:

Mantle + Contaminant = Bushveld
$$(1-X_{cont})^*[S]_{mantle} * \Delta^{33}S_{mantle} + (X_{cont})^*[S]_{cont} * \Delta^{33}S_{cont} = [S]_{BV} * \Delta^{33}S_{BV}$$

$$(1)$$

(where X_{cont} = percent contaminant, $[S]_{mantle}$ = concentration of sulfur in mantle, $\Delta^{33}S_{mantle}$ = the $\Delta^{33}S$ isotopic composition of the mantle, $[S]_{cont}$ = concentration of sulfur in the contaminant, $[S]_{BV}$ = concentration of sulfur in the Bushveld, and $\Delta^{33}S_{BV} = \Delta^{33}S$ isotopic composition of the Bushveld. Values used to constrain the mixing model include: $\Delta^{33}S_{mantle} = 0$, $[S]_{BV} = 800$ ppm (Cawthorn, 2005), $\Delta^{33}S_{BV} = .11$ (average value reported from Bushveld igneous rocks by Penniston-Dorland et al., 2008))

Since the Δ^{33} S value of the mantle is reported to be zero, the equation reduces to:

$$(X_{cont})^*[S]_{cont} * \Delta^{33}S_{cont} = [S]_{BV} * \Delta^{33}S_{BV}$$
 (2)

By manipulating this equation, one can come up with an equation for the percentage of contaminant needed based on a particular value of the concentration of sulfur within the contaminant. This equation thus becomes:

$$X_{cont} = (([S]_{BV} * \Delta^{33}S_{BV}) / ([S]_{cont} * \Delta^{33}S_{cont}))$$
 (3)

where $[S]_{cont}$ = between 20 and 450 ppm for peridotite xenoliths (Maier et al. 2005), and $\Delta^{33}S_{cont}$ = measured value.

A way to visualize this is as a single contamination curve, representing the xenoliths, mantle, Bushveld Complex, and another likely source of contamination. The line represents a mixture of the contaminant (any point along the line to the right of the Bushveld data point) with both a high Δ^{33} S value and high concentration of sulfur. Anything that falls along this line can be explained by using the lever rule, by calculating what percent of each endmember of the line is responsible for the mixture noticed. Here, the Bushveld complex is the contaminated mixture that is in question. The peridotite xenoliths, however, are not even close to this mixing curve and even if they were, their values are much too small to account for the values reported in the Bushveld Complex.

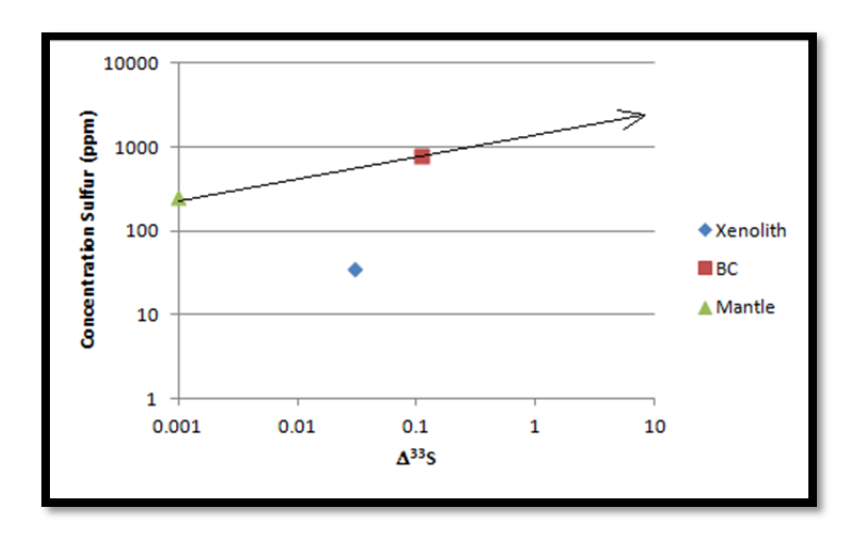


Figure 14 This plot shows the relative values of Δ^{33} S and concentration of sulfur for each of three different sources; xenoliths (SCLM), Bushveld igneous rocks, and mantle. The line connecting the mantle and Bushveld igneous rock values shows indicates that a possible contaminant will need to fall along this line to the right of the Bushveld value; the further to the right along the mixing line, the less percentage of the contaminant is needed to account for the signature displayed by the **Bushveld Complex. All values are** reported as averages.

Another way to interpret this is to use a trivariate system, manipulating measured D33S values, concentration of sulfur within the sample, and the percentage of the mantle + contaminant that needs to be the contaminant. Measured $\Delta^{33}S$ values for the mantle xenoliths or other possible contaminants may be plugged into equation 3 and followed on the curve set. Whichever curve it intersects, the corresponding value on the y-axis indicates the percentage of contamination needed to yield the amount of contamination seen in the Bushveld. For example, if a xenolith were to have a $\Delta^{33}S$ value of 2‰, then a straight vertical line would be drawn on the graph at that point. The sulfur concentration would need to be measured, and depending on what that was, a horizontal line would be drawn from that concentration curve. Wherever that intersects the y-axis determines the amount of contamination needed to plausibly be responsible for the Bushveld signature. For this example, if that xenolith had a sulfur concentration of 100 ppm, then the percentage of the mantle material would need to be about 45% contaminant in order to produce the anomalous signature.

However, since the data attained from the xenolith samples averaged .03, these values represent an implausibly high amount (over 100%) of contamination needed to be responsible for the Bushveld signature. Even sample PHN 5247, that had a Δ^{33} S value of .144, still is too small to produce the contamination signature (within the constraints of 20 to 450 ppm). Therefore, it is concluded that the contamination seen in the Bushveld is in fact not a direct consequence of contamination by a sub-continental lithospheric mantle, but rather contamination from different source.

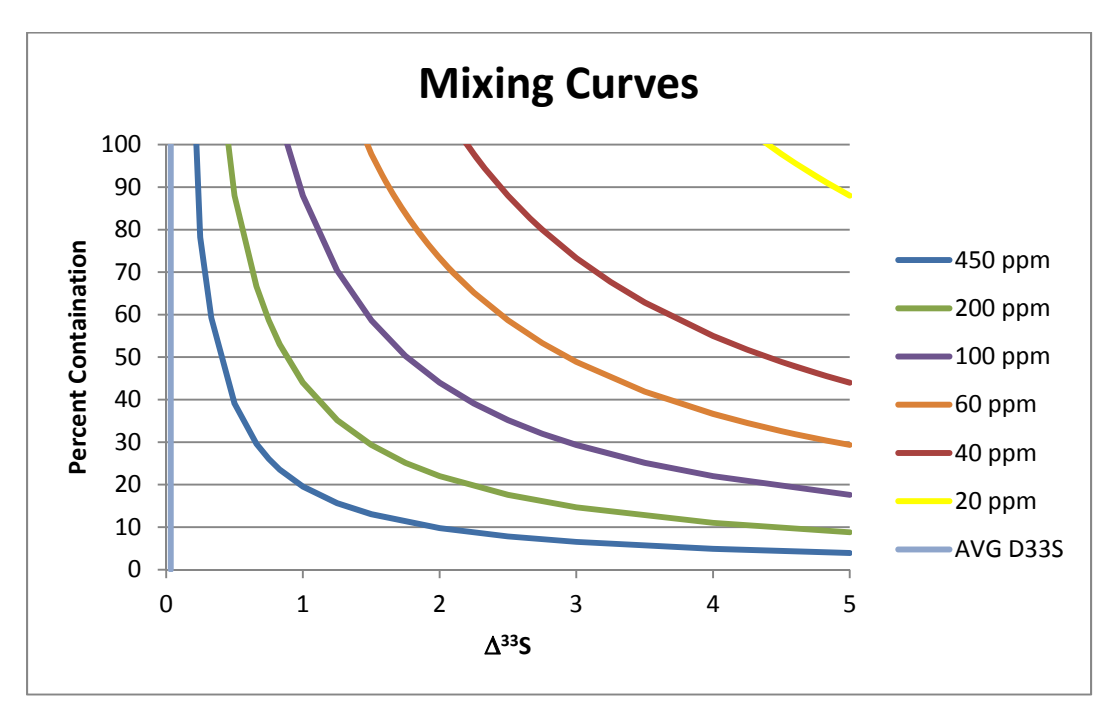


Figure 15 Mixing curves of percent contamination needed per Δ^{33} S value, with my average xenolith data as a straight line (range of measured Δ^{33} S values for peridotite xenoliths), indicating that it is impossible for these to be a source of contamination of the Bushveld since it does not intersect any of the curves (ie. more than 100% of contaminant is needed)

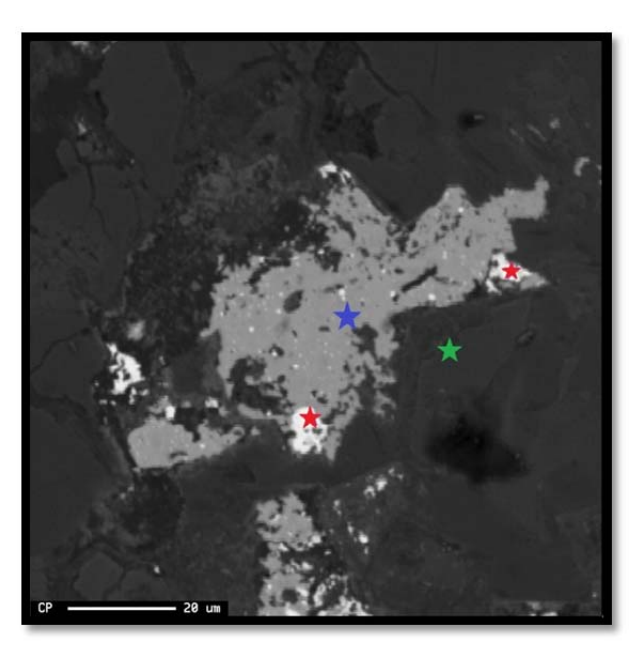


Figure 14 BSE image of celsian grain (blue star) with barite phases (red stars) and surrounding spinel (green star). Scale bar is 20 μm

7.5 Implications

7.5.1 Thode analyses

I chose to run Thode reductions on multiple samples for a few reasons. Firstly, when analyzing the thin sections of a few of the samples under back scattered electrons (BSE), sulfate phases were found within sample FRB 1655. The BSE image below shows a single grain of what was reported to be celsian, a barium feldspar with a formula of BaAl₂Si₂O₈. This can be seen in the photo as the blue star. Along with this barium rich phase, two grains of barite were found on the edges of this mineral as indicated by the red stars.

Since barite was already found in sample FRB 1655, I decided to run a Thode reduction in order to see how much sulfate was in the

xenolith. I used 2.2 grams of rock powder, which is about the sample amount that I used to reduce the other samples via CRS reduction, and a sufficient amount of silver sulfide was extracted from the powder in order to be analyzed on the mass spectrometer. I then carried out another entire Thode reduction line, reducing five more samples (3 peridotites, 1 eclogite, and 1 kimberlite) and all of these samples yielded sufficient product. It is interesting in that all the samples (peridotites, eclogites, and kimberlites) maintain roughly the same amount of sulfate within them, which may have implications for the original source of these materials.

The second reason why Thode analyses have been conducted were to provide more information about how these xenoliths acquired their anomalous signature. The fact that there are eclogite xenoliths coming from the sub-continental lithospheric mantle along with normal peridotite xenoliths, implies that these were either formed by subduction related processes or that the overlying continental lithosphere subjected the protolith to sufficient temperatures and pressures to cause metamorphism to occur. If subduction, however, was the likely scenario for how these eclogite xenoliths were formed, this may imply that ancient ocean sulfate from crustal sedimentary rocks have been recycled back into the lithospheric mantle. Ancient oceanic sulfate is proposed to have a Δ^{33} S value that is negative, and if enough of this material was incorporated into the peridotite and eclogite xenoliths as they were formed / emplaced, this may have affected their isotopic signatures. The significance of this is that the results could yield false positive, where the values attained are very low, positive values, when they could actually be very high positive values. For example, if the xenoliths in the SCLM originally had very high Δ^{33} S values. but interacted with oceanic sulfate sources as they were being emplaced, and incorporated a large negative value, this could ultimately change the sulfur isotopic composition of the xenoliths to have a close to zero value. However, the intrinsic Δ^{33} S value of these xenoliths was actually high. Since these are representative of the magma source in the SCLM, having a truly high Δ^{33} S

value could suggest that they are actually the source of the anomalous signature in the Bushveld Complex, whereas just the data that has been gathered (Δ^{33} S of the xenoliths is close to zero) rejects the hypothesis that they are the likely source of contamination. Thus, I believe it is important to the conclusions of this study that sulfate reductions occur and multiple isotopic analyses be provided by the sulfate phases of these rocks. Unfortunately, the data from these reductions was not collected, but once the data has been collected, new insights may be added to this study.

7.5.2 Kimberlite

Kimberlite analyses were added to this study to determine whether the peridotite and eclogite xenoliths could have been contaminated due to interaction with the kimberlite magma on ascent. $\Delta^{33}S$ values from these samples may help to elucidate possibilities of how the xenoliths acquired their signatures. However, CRS reductions have been conducted the kimberlite samples, and nearly no silver sulfide was formed as product, implying that the kimberlite material has a very low abundance of sulfide phases. This is interesting because the xenoliths from the SCLM had sufficient amounts of sulfide, yet the material that transported them to the surface did not. Since kimberlite eruptions are often violent due to the high abundance of volatiles, one would think that they would incorporate much of the surrounding material as it ascends to the surface. Although the samples lacked significant amounts of sulfide, this does not rule out the possibility that the xenoliths samples interacted with the kimberlite and became contaminated. If the $\Delta^{33}S$ values from the sulfate phases within the kimberlite are high negative values, then this may have been incorporated into the xenoliths, lowering their intrinsic $\Delta^{33}S$ values.

8 Conclusion

The Bushveld Complex in South Africa has very unique characteristics including its isotopically anomalous layered igneous intrusion, its size, and its platinum group element content. Many models have been suggested to explain its isotopically anomalous features; however, the data from this project reject the possibility of contamination from the sub-continental lithospheric mantle as a source of the anomalous Δ^{33} S isotopic composition of Bushveld rocks.

The significance of this project lies in the fact that the results will shed light upon various processes, such as how large layered igneous intrusion form, and even provide insight into the ancient sulfur cycle. This is also the first study to conduct measurements on Δ^{33} S values from xenoliths from the Premier kimberlite. By understanding the ultimate magma source for this intrusion, we can then begin to understand the processes of PGE mineralization better. This is important both from a geologic and economic perspective.

Seen in Figure 1 from the beginning of this paper, the yellow area on the diagram depicts the Bushveld Complex with an average Δ^{33} S value of .11. The green area shows the possible source of contamination, the SCLM, and the red area is the asthenospheric mantle, with a Δ^{33} S of zero. Intuition alone tells us that no matter how much of the green material (SCLM) is mixed with the red material (asthenospheric mantle) along its ascent, they cannot together create the signal demonstrated by the overlying Bushveld Complex. Even if there were no magma present (100%)

contaminant of the SCLM), the $\Delta^{33}S$ value would only be .03, and cannot therefore reach .11 as seen in the Bushveld Complex.

The results of this project have suggested that while some of the xenoliths carry a nonzero $\Delta^{33}S$ signature, it is not sufficient to be responsible for the anomalous $\Delta^{33}S$ signature of the Bushveld Complex. Thus, the SCLM is not a likely source of contamination. Further investigations should now be conducted to test other possible sources for contamination of the Bushveld Complex, since this project has successfully ruled out one of the most attractive hypotheses. The next logical investigation should be in regards to contamination upon emplacement by the Transvaal Supergroup crustal rocks. These sedimentary rocks may have high enough $\Delta^{33}S$ values and sulfur concentration to be responsible for the anomalous $\Delta^{33}S$ signature found within the Bushveld Complex. Further analysis of sulfate phases should also be investigated, in both xenoliths and kimberlite samples in order to provide a better understanding of their interaction upon ascent.

9 Acknowledgements

I would especially like to thank my advisor Dr. Penniston-Dorland for devoting so much time and effort in guiding me in this research project. I would like thank my other co-advisor, Dr James Farquhar, for not only helping me to understand project details, but for also allowing me to use his lab facility, equipment, and chemicals needed to carry out this experiment. Dr. P-D and I are also grateful to have received these xenolith samples from the Smithsonian Museum of Natural History with the help of our contacts Dr. Sorena Sorensen and Leslie Hale. Thanks also to Dr. Phil Piccoli for assistance on the electron microprobe and thanks to Daniel Eldridge for helping me with the fluorination and mass spectrometry part of the project.

10 References

- Carlson, R.W., Boyd, F.R., Shirey, S.B., Janney, P.E., Grove, T.L., Bowring, S.A., Schmitz, M.D., Dann, J.C., Bell, D.R., Gurney, J.J., Richardson, S.H., Tredoux, M., Menzies, A.H., Pearson, D.G., Hart, R.J., Wilson, A.H., Moser, D., 2000, Continental Growth, Preservation, and Modification in Southern Africa, GSA Today, 10, 1-7.
- Cawthorn, R. G., 2005, Pressure fluctuations and the formation of the PGE-rich Merensky and chromitite reefs: Bushveld Complex, Mineralium Deposita, 40, 231-235.
- Farquhar, J., Bao, H.M., and Thiemens, M., 2000, Atmospheric influence of Earth's earliest sulfur cycle, Science, 289, 756-758.
- Farquhar, J., Wing, B.A., McKeegan, K.D., Harris, J.W., Cartigny, P., and Thiemens, M.H., 2002, Mass-independent sulfur of inclusions in diamond and sulfur recycling on early Earth, Science, 298, 2369-2372.
- Gregoire, M., Tinguely, C., Bell, D.R., le Roex, A.P., 2005, Spinel lherzolite xenoliths from the Premier kimberlite (Kaapvaal craton, South Africa): Nature and evolution of the shallow upper mantle beneath the Bushveld complex, Lithos, 84, 185-205.

- Harris, C., Pronost, J.J.M., Ashwal, L.D., and Cawthorn, R.G., 2005, Oxygen and hydrogen isotope stratigraphy of the Rustenberg Layered Suite, Bushveld Complex: Constraints on crustal contamination, Journal of Petrology, 46, 579-601.
- Hatton, C.J., Sharpe, M.R., 1989, Significance and origin of boninite-like rocks associated with the Bushveld Complex. In: Crawford, A.J. (Ed.), Boninites and Related Rocks. Unwin Hyman, London, pp. 174-208.
- Hiebert, R.S., and Bekker, A., 2010, Multiple Sulfur Isotopes: A New Tool for Identification of Sulfur Source in Magmatic Sulfide Deposits, Ontario Geological Survey, 269, 1-4.
- Kruger, F.J., 1994, The Sr isotope stratigraphy of the western Bushveld Complex, South African Journal of Geology, 97, 393-398.
- Maier, W.D., Arndt, N.T., and Curl, E.A., 2000, Progressive crustal contamination of the Bushveld Complex: Evidence from Nd isotopic analyses of the cumulate rocks, Contributions to Mineralogy and Petrology, 140, 316-327.
- Maier, W.D., Arndt, N.T., Curl, E.A., 2000. Progressive crustal contamination of the Bushveld Complex: evidence from Nd isotopic analyses of the cumulate rocks. Contributions to Mineralogy and Petrology 140, 316-327.
- Maier, W.D., Peltonen, P., Juvonen, R., and Pienaar, C., 2005, Platinum-group elements in peridotite xenoliths and kimberlite from the Premier kimberlite pipe, South Africa, South African Journal of Geology, 108, 413-428.
- McCandless, T.E., Ruiz, J., Adair, B.I., Freydier, C., 1999. Re-Os and Pd/Ru variations in chromitites from the Critical Zone, Bushveld Complex, South Africa. Geochemica et Cosmochimca Acta 63, 911-923.
- Penniston-Dorland, S.C., Wing, B.A., Nex, P.A.M., Kinnaird, J.A., Farquhar, J., Brown, M., Sharman, E.R., 2008, Multiple sulfur isotopes reveal a magmatic origin for the Platreef platinum group element deposit, Bushveld Complex, South Africa, Geology, 36, 979-982.
- Peters, M., Strauss, H., Farquhar, J., Ockert, C., Eickmann, B., Jost, C. L., 2010, Sulfur cycling at the Mid-Atlantic Ridge: A multiple sulfur isotope approach, Chemical Geology, 269, 180-196.
- Richardson, S.H. and Shirey, S.B., 2008, Continental mantle signature of Bushveld magmas and coeval diamonds, Nature, 453, 910-913.
- Sakai, H., Des Marais, D. J., Ueda, A., Moore, J. G., 1984, Concentrations and isotope ratios of carbon, nitrogen, and sulfur in ocean-floor basalts, Geochimica et Cosmochimica, 48, 2433-2441.
- Smith, C.B., 1983, Rubidium-Strontium, Uranium-Lead and Samarium-Neodymium isotopic studies of kimberlite and selected mantle-derived xenoliths, Unpublished PhD thesis, University Witwatersrand, Johannesburg, South Africa.

- Thomassot, E., Cartigny, P., Harris, J.W., Lorand, J.P., Rollion-Bard, C., and Chaussidon, M., 2009, Metasomatic diamond growth: A multi-isotope study (13C, 15N, 33S, 34S) of sulphide inclusions and their host diamonds from Jwaneng (Botswana), Earth and Planetary Science Letters, 282, 79-90.
- Vaughan, David J., ed. Sulfide Mineralogy and Geochemistry. Vol. 61. Chantilly, VA: Mineralogical Society of America, 2006. Print.
- Zheng, Y. F., 1992, Sulfur isotopes in the mantle, Natur Wissenshaften, 79, 511-512.